

Quantum Simulation of Energy Bifurcation and \mathbb{Z}_2 -Symmetry Restoration in Macroscopic Quantum Tunneling

Masao Hirokawa*
(Dated: May 25, 2026)

Macroscopic quantum tunneling (MQT), a cornerstone of Leggett’s program, is deeply linked with instanton physics, yet its experimental verification remains elusive. This Perspective demonstrates that the quantum Rabi model manifests observable, instanton-like effects via quantum simulation. In the MQT regime, qubit-boson interactions drive Polyakov’s energy bifurcation, governing tunneling and spontaneous symmetry breaking. Mapping the quantum Rabi model onto an effective double-well potential reveals that while tunneling suppression induces spontaneous symmetry breaking, instanton-like contributions act to restore it. This mechanism enables experimental access to the classical Euclidean action of an effective instanton-like particle, offering a route to probe non-perturbative phenomena.

I. INTRODUCTION

The investigation of macroscopic quantum phenomena is often referred to as Leggett’s program [1–3], with macroscopic quantum tunneling (MQT) [4–7] serving as a prime example. The quantum Rabi model can be regarded as a representation of MQT via a unitary transformation, since it models the two-level approximation of tunneling between two symmetric wells in a double-well potential (see Section II). In light of the MQT features revealed by this model, it is instructive to revisit Polyakov’s statement in Ref.[8] (p.430): “*Our main idea is that in cases with superficially broken symmetry there may exist certain classical trajectories which repair the symmetry. The simplest example of this is two symmetrical wells separated by a barrier in quantum mechanics. In this case, if we neglect the small penetration effect we obtain a degenerate vacuum and broken symmetry. Taking into account trajectories connecting the two wells removes this degeneracy. These trajectories will be called pseudoparticles or instantons.*” Indeed, an instanton-like effect emerges in the ground state energy of the quantum Rabi model [9], which challenges Polyakov’s assertion (see Fig.1 and Section 4). The quantum Rabi model can often be realized in quantum simulators [10–13]. In this context, quantum simulation refers to the implementation of a quantum phenomenon with a programmable quantum system. The technology of quantum simulators has been advancing continuously over the last 20 years [10–23].

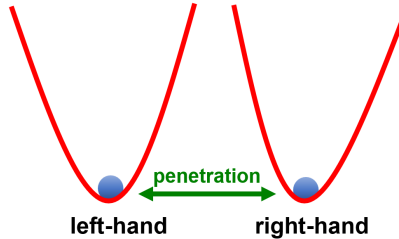


FIG. 1. The system with two symmetric well potentials but no penetration exhibits degenerate ground states, leading to spontaneous symmetry breaking. However, once tunneling between the wells is incorporated, the symmetry is restored through the introduction of pseudo-particles known as instantons.

Consider the ground state of a macroscopic quantum system with a symmetric double-well potential separated by a barrier. We assume that the Hamiltonian of the macroscopic system possesses symmetry, hereafter referred to as the *macrosystem Hamiltonian* in accordance with Ref.[3]. The penetration (and thus tunneling) is absent as the barrier between the two wells becomes infinitely high. As is well known, the ground state becomes degenerate, implying that the symmetry is spontaneously broken. According to Polyakov, instantons emerge to restore the symmetry by enabling tunneling between the wells. This restoration lifts the degeneracy, splitting the ground states into a new ground state and a first excited state [24–26]. In this Perspective, we refer to this energy splitting as *Polyakov’s energy bifurcation*.

* hirokawa@inf.kyushu-u.ac.jp; Graduate School of Information Science and Electrical Engineering, Kyushu University, 744 Motooka, Nishi-ku, Fukuoka, 819-0395, Japan; Quantum Computing System Center, Kyushu University, 744 Motooka, Nishi-ku, Fukuoka, 819-0395, Japan; Quantum and Spacetime Research Institute, Kyushu University, 744 Motooka, Nishi-ku, Fukuoka, 819-0395, Japan

The macrosystem Hamiltonian is described by the Schrödinger operator with the symmetric double-well potential $V(x)$ [3]:

$$H_{\text{MS}} = \frac{1}{2}\hat{p}^2 + V(\hat{x}), \quad (1)$$

where \hat{x} and \hat{p} are respectively the operators of position x and momentum p satisfying the canonical commutation relation, $[\hat{x}, \hat{p}] = i\hbar$. The potential $V(x)$ has two symmetrical wells. We assume that the minima of the wells are separated, as shown in Fig.2, and that the quantum motion of the particle in each well is semiclassical. While this physical system is called an ‘‘intrinsically two-state system’’ in Ref.[2], we call it a *two-level system* in this Perspective. The states of the semiclassical particle in the left-hand and right-hand wells are respectively approximated by two states of the two-level system: the ground state and the first excited state. Systems with two macroscopic states, like ammonia molecules, are often described using a two-level system (see III-10-1 of Ref.[27], as well as Refs.[2, 3, 28–32]). Thus, we consider this two-level system to represent a particle localized in either of the two individual minima. In Ref.[2], by choosing the basis such that the eigenstates of the Z -gate σ_z correspond to the states localized in the left and right wells, the energy of the two-level system is described by the Hamiltonian $-\frac{\hbar\omega_a}{2}\sigma_x + \frac{1}{2}\varepsilon\sigma_z$. The first term describes tunneling between the two wells mediated by the X -gate σ_x , whereas the second term introduces an energy bias.

Let us consider a double-well potential $V(x)$ with two symmetrical wells having minima at $x = \pm x_0$ (see Fig.2). Following Ref.[3], we approximate the potential $V(x)$ as $V_{x_0}(x) = \frac{\omega_c^2}{2}(x \mp x_0)^2$ near $x = \pm x_0$, where ω_c is the frequency of the single-mode boson. Thus, for x sufficiently close to $\pm x_0$, the macrosystem Hamiltonian H_{MS} can be approximated as

$$H_{\text{MS}} \approx \frac{1}{2}\hat{p}^2 + V_{x_0}(\hat{x}).$$

We denote the right-hand side of this approximation by $H_{\text{MS}}^{\text{ho}}(\omega_c, \pm x_0)$. However, approximating the original macrosys-

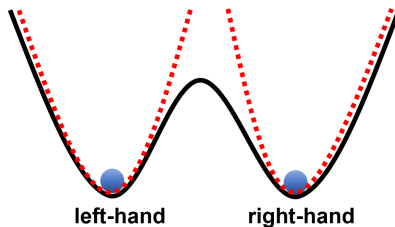


FIG. 2. The graph shows a double-well potential $V(x)$.

tem Hamiltonian H_{MS} solely with the harmonic oscillator Hamiltonians $H_{\text{MS}}^{\text{ho}}(\omega_c, \pm x_0)$ is insufficient, since the harmonic oscillator potentials confine the particles. Therefore, an interaction term is required to account for the tunneling between the two wells. We derive this by mapping the quantum Rabi model onto an effective double-well potential, rendering the well-known analogy with the ground-state energy bifurcation explicit (see Fig.3 and Section II).

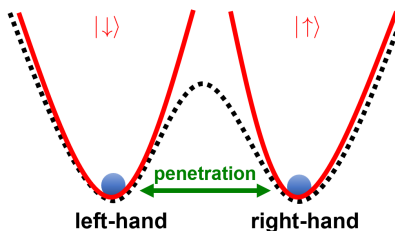


FIG. 3. This figure illustrates a two-level approximation of the double-well potential $V(x)$. The Hamiltonian for the red part is given by $\begin{pmatrix} 0 & 0 \\ 0 & 1 \end{pmatrix} \otimes H_{\text{MS}}^{\text{ho}}(\omega_c, -x_0)$ and $\begin{pmatrix} 1 & 0 \\ 0 & 0 \end{pmatrix} \otimes H_{\text{MS}}^{\text{ho}}(\omega_c, +x_0)$. The penetration (shown in green) is formed as described in Section II.

The quantum Rabi model exhibits stable spontaneous \mathbb{Z}_2 -symmetry breaking in a certain limit (see Section III). In the specific case where the qubit transition and the single-mode boson frequencies are strictly matched, the \mathbb{Z}_2 -symmetry breaking transition corresponds to the transition from $\mathcal{N} = 2$ supersymmetry (SUSY) to its spontaneous

breaking [33, 34]. As shown in Fig.4, in the strong-coupling limit ($g \rightarrow \infty$), where g is the coupling strength between the qubit and the single-mode boson, all eigenstates become nearly two-fold degenerate. Furthermore, the eigenenergies are spaced at almost equal intervals and diverge toward negative infinity, following a common parabolic trend of $-c_0 g^2$. The constant c_0 is determined by the self-energy of the single-mode boson's self-interaction (see Section III). This behavior results in spontaneous \mathbb{Z}_2 -symmetry breaking. The right panels of Fig.4 show the special case where the qubit transition frequency and the single-mode boson frequency are equal. At $g = 0$, the ground state energy is simple (i.e., the ground state is unique), while all excited states are two-fold degenerate. The eigenenergies are distributed at equal intervals, resulting in $\mathcal{N} = 2$ SUSY. Viewed from the strong-coupling limit ($g \rightarrow \infty$) where spontaneous SUSY breaking occurs, the $\mathcal{N} = 2$ SUSY emerges at much higher energy levels, as illustrated in Fig.4. This transition has been mathematically proven for the renormalized quantum Rabi Hamiltonian [33] (see Section III) and experimentally demonstrated using an ion-trap simulator [12].

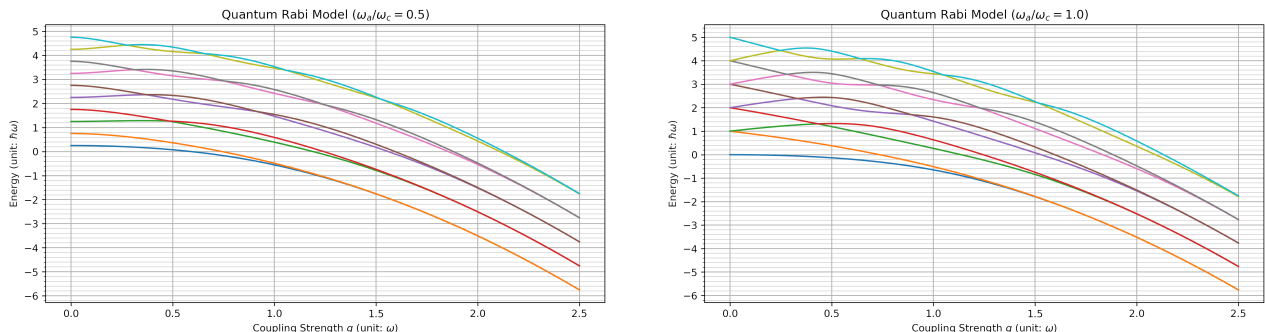


FIG. 4. Energy levels of the lowest ten states in the quantum Rabi model as a function of the coupling strength g . The left and right panels show the cases for $\omega_a = 0.5\omega$, $\omega_c = \omega$ and $\omega_a = \omega_c = \omega$, respectively, where ω is a constant frequency. Here, ω_a denotes the qubit transition frequency and ω_c is the frequency of the single-mode boson.

The contents of this Perspective are organized as follows: In Section II, we introduce a unitary transformation that maps the quantum Rabi model to a unitarily equivalent representation, termed the *transformed quantum Rabi model*. This mapping provides a physical interpretation of the unbiased ($\varepsilon = 0$) two-level system Hamiltonian with a qubit-boson interaction, thereby positioning the quantum Rabi model as a two-level approximation of the double-well potential. Building on the framework established in Refs.[2, 4, 28–30, 35], Ref.[9] briefly introduces a two-level-system approximation using the transformed quantum Rabi model. In Section III, we clarify the physical mechanism of the transition to spontaneous \mathbb{Z}_2 -symmetry breaking in terms of the interaction in the transformed quantum Rabi model. In Section IV, based on the results for the classical Euclidean action of an effective instanton-like particle [9], we show that the transformed quantum Rabi model reveals Polyakov's energy bifurcation. Furthermore, by leveraging this bifurcation, we propose a formula for experimentally observing the classical Euclidean action of the effective instanton-like particle.

II. TRANSFORMED QUANTUM RABI MODEL AND EFFECTIVE DOUBLE-WELL POTENTIAL

The state space of a qubit is \mathbb{C}^2 , the 2-dimensional unitary space, where \mathbb{C} is the set of all the complex numbers. The up-spin state and the down-spin state are denoted by $|\uparrow\rangle = \begin{pmatrix} 1 \\ 0 \end{pmatrix}$ and $|\downarrow\rangle = \begin{pmatrix} 0 \\ 1 \end{pmatrix}$, respectively. The state space of a single-mode boson is given by the boson Fock space \mathcal{F}_b , spanned by all the Fock states $|n\rangle$, $n = 0, 1, 2, \dots$. We define the total state space of the system as the Hilbert space $\mathcal{F} = \mathbb{C}^2 \otimes \mathcal{F}_b$. The standard Pauli matrices are denoted by $\sigma_x = \begin{pmatrix} 0 & 1 \\ 1 & 0 \end{pmatrix}$, $\sigma_y = \begin{pmatrix} 0 & -i \\ i & 0 \end{pmatrix}$, and $\sigma_z = \begin{pmatrix} 1 & 0 \\ 0 & -1 \end{pmatrix}$. The annihilation and creation operators of the single-mode boson are denoted by a and a^\dagger , respectively. We use the notation '1' for the 2×2 identity matrix, the identity operator on \mathcal{F}_b , and the numerical value 1. We often omit the tensor product symbol ' \otimes ' and write the state $|\#\rangle \otimes |\psi\rangle$ as $|\#\rangle |\psi\rangle$ for the states $|\#\rangle \in \mathbb{C}^2$ and $|\psi\rangle \in \mathcal{F}_b$. Correspondingly, an operator $A \otimes B$ acting on \mathcal{F} is abbreviated as AB , where the operators A and B act on \mathbb{C}^2 and \mathcal{F}_b , respectively. In addition, we often omit '1' and ' $\otimes 1$,' writing $A \otimes 1$ as A and $1 \otimes B$ as B .

The unitary equivalence, $\mathbb{C}^2 \otimes \mathcal{F}_b \cong \mathcal{F}_b \oplus \mathcal{F}_b$, obtained by the correspondence,

$$\mathbb{C}^2 \otimes \mathcal{F}_b \ni |\uparrow\rangle \otimes |\psi\rangle + |\downarrow\rangle \otimes |\varphi\rangle \longleftrightarrow \begin{pmatrix} |\psi\rangle \\ |\varphi\rangle \end{pmatrix} \in \mathcal{F}_b \oplus \mathcal{F}_b,$$

allows us to identify the operator, $(|\uparrow\rangle\langle\uparrow| \otimes B_1 + (|\uparrow\rangle\langle\downarrow| \otimes B_2 + (|\downarrow\rangle\langle\uparrow| \otimes B_3 + (|\downarrow\rangle\langle\downarrow| \otimes B_4$ acting on \mathcal{F} with the operator matrix $\begin{pmatrix} B_1 & B_2 \\ B_3 & B_4 \end{pmatrix}$ acting on $\mathcal{F}_b \oplus \mathcal{F}_b$, where B_i , $i = 1, 2, 3, 4$, are operators on \mathcal{F}_b .

The Hamiltonian of the quantum Rabi model reads

$$H_{\text{QR}} = \frac{\hbar\omega_a}{2}\sigma_z + \hbar\omega_c \left(a^\dagger a + \frac{1}{2} \right) + \hbar g \sigma_x (a + a^\dagger),$$

characterized by the qubit transition frequency ω_a , the single-mode-boson frequency ω_c , and the coupling strength $g \geq 0$. Here, \hbar is the Planck constant divided by 2π . Let us define the parity operator P , associated with the spin localization and the boson number, by $P = \sigma_z(-1)^{a^\dagger a}$. Then, the parity symmetry of the quantum Rabi Hamiltonian is immediately evident:

$$[H_{\text{QR}}, P] = 0. \quad (2)$$

By introducing the position operator (i.e., single-mode scalar field) $\hat{x} = \sqrt{\frac{\hbar}{2\omega_c}}(a + a^\dagger)$ and the momentum operator (i.e., the conjugate field) $\hat{p} = -i\sqrt{\frac{\hbar\omega_c}{2}}(a - a^\dagger)$, which act on the boson Fock space \mathcal{F}_b , the quantum Rabi Hamiltonian can be rewritten as

$$H_{\text{QR}} = \frac{\hbar\omega_a}{2}\sigma_z + H_{\text{MS}}^{\text{ho}}(\omega_c, 0) + g\sqrt{2\hbar\omega_c}\sigma_x\hat{x}, \quad (3)$$

where $H_{\text{MS}}^{\text{ho}}(\omega_c, 0) = \frac{1}{2}\hat{p}^2 + \frac{\omega_c^2}{2}\hat{x}^2$.

We consider a unitary transformation of the quantum Rabi Hamiltonian H_{QR} . For the unitary operator $U_0 = \frac{1}{\sqrt{2}} \begin{pmatrix} 1 & -1 \\ 1 & 1 \end{pmatrix}$, the transformed Hamiltonian is expressed as

$$U_0^* H_{\text{QR}} U_0 = -\frac{\hbar\omega_a}{2}\sigma_x + H_{\text{MS}}^{\text{ho}}(\omega_c, 0) + g\sqrt{2\hbar\omega_c}\sigma_z\hat{x}. \quad (4)$$

Consequently, the transformed Hamiltonian $U_0^* H_{\text{QR}} U_0$ is the single-mode version of the spin-boson Hamiltonian presented in Eq.(1.4) of Ref.[2]. Following the physical interpretation in Ref.[2], in the σ_z -representation, the X -gate σ_x acts as the tunneling matrix exchanging the two states. Furthermore, the coupling strength g serves as a parameter representing the distance between the two minima of the symmetric double-well potential. Although the harmonic oscillators of the spin-boson model in Ref.[2] consist of infinitely many modes (representing a heat bath), our transformed Hamiltonian $U_0^* H_{\text{QR}} U_0$ interacts with only a single-mode harmonic oscillator. Therefore, we assign it a distinct physical interpretation. We consider the separation of the symmetric wells in a double-well potential [36]. As noted in Refs.[2, 37], a symmetric double-well potential can approximate a qubit (i.e., a two-level system), a concept essential for implementing qubits in superconducting circuits. Here, we introduce an approximation in which these roles are reversed. Although the two-level system is conventionally assumed to be coupled to a heat bath described by a Bose field in the Caldeira-Leggett model [4, 35], we reexamine the Hamiltonian given by Eq.(4) in light of Coleman's idea [24–26].

As reported in Refs.[38–41], the wavefunction of a Schrödinger or Dirac particle may acquire a phase factor at the barrier boundary during tunneling. We show below that a similar phenomenon occurs in the quantum Rabi model. To do this, we introduce two unitary operators. We define the unitary operator U_1 by $U_1 = \begin{pmatrix} \exp[-i\frac{\pi}{2}a^\dagger a] & 0 \\ 0 & \exp[-i\frac{\pi}{2}a^\dagger a] \end{pmatrix}$. It is noteworthy that the transformation by the diagonal component operator performs a type of Fourier transform:

$$\begin{cases} e^{i\frac{\pi}{2}a^\dagger a}\hat{x}e^{-i\frac{\pi}{2}a^\dagger a} = \frac{1}{\omega_c}\hat{p}, \\ e^{i\frac{\pi}{2}a^\dagger a}\hat{p}e^{-i\frac{\pi}{2}a^\dagger a} = -\omega_c\hat{x}. \end{cases} \quad (5)$$

We define the unitary operator U_ϕ by $U_\phi = \begin{pmatrix} e^{-i\frac{\pi}{\omega_c}(a^\dagger+a)} & 0 \\ 0 & e^{i\frac{\pi}{\omega_c}(a^\dagger+a)} \end{pmatrix}$. Then, our Hamiltonian of the transformed quantum Rabi model is given by

$$\tilde{H}_{\text{QR}} = (U_0 U_1 U_\phi)^* H_{\text{QR}} (U_0 U_1 U_\phi).$$

We first note that $(U_0 U_1 U_\phi)^*(\mathbb{C}^2 \otimes \mathcal{F}_b) = \mathbb{C}^2 \otimes \mathcal{F}_b$, which is the state space of a qubit and a single-mode Bose quasi-particle. As shown in Section 2 of Ref.[34], for the grading operator $N_F = -\sigma_z$, a bosonic state is given by $|\downarrow\rangle|\psi\rangle$ for $\psi \in \mathcal{F}_b$ such that $N_F |\downarrow\rangle|\psi\rangle = |\downarrow\rangle|\psi\rangle$; thus, the space of bosonic states is $\mathcal{F}_\downarrow = |\downarrow\rangle\mathcal{F}_b$. Meanwhile, a fermionic state is given by $|\uparrow\rangle|\psi\rangle$ for $\psi \in \mathcal{F}_b$ such that $N_F |\uparrow\rangle|\psi\rangle = -|\uparrow\rangle|\psi\rangle$, and the space of fermionic states is $\mathcal{F}_\uparrow = |\uparrow\rangle\mathcal{F}_b$.

The total state space is decomposed into the orthogonal sum of the bosonic-state and fermionic-state spaces; hence, the decomposed state space is unitarily equivalent to the orthogonal sum of the two single-mode Fock spaces,

$$\mathbb{C}^2 \otimes \mathcal{F}_b = \mathcal{F}_\downarrow \oplus \mathcal{F}_\uparrow \cong \mathcal{F}_b \oplus \mathcal{F}_b, \quad (6)$$

through the correspondences,

$$\begin{pmatrix} c_1 \\ c_2 \end{pmatrix} \otimes \varphi = |\downarrow\rangle \otimes c_2 |\varphi\rangle \oplus |\uparrow\rangle \otimes c_1 |\varphi\rangle \cong \begin{pmatrix} c_1 \varphi \\ c_2 \varphi \end{pmatrix} = \begin{pmatrix} \psi_1 \\ \psi_2 \end{pmatrix},$$

where $c_1, c_2 \in \mathbb{C}$, $\varphi \in \mathcal{F}_b$, and $\psi_1 = c_1 \varphi, \psi_2 = c_2 \varphi \in \mathcal{F}_b$. Then, the spin-annihilation operator $\sigma_- = \frac{1}{2}(\sigma_x - i\sigma_y)$ and spin-creation operator $\sigma_+ = \frac{1}{2}(\sigma_x + i\sigma_y)$ describe particle tunneling between the bosonic-state space \mathcal{F}_\downarrow and the fermionic-state space \mathcal{F}_\uparrow . Furthermore, the two single-mode Fock spaces \mathcal{F}_b on the right-hand side of Eq.(6) can be identified with $L^2(-\infty, -\Lambda)$ and $L^2(+\Lambda, +\infty)$ for a constant $\Lambda \geq 0$, respectively. Consequently, we obtain the state space for the wavefunctions, $L^2(-\infty, -\Lambda) \oplus L^2(+\Lambda, +\infty) \cong L^2(\mathbb{R} \setminus [-\Lambda, +\Lambda])$, where the interval $[-\Lambda, +\Lambda]$ effectively acts as a barrier for the wavefunctions [38–42].

Setting the operators A and B as

$$A = \begin{pmatrix} H_{\text{MS}}^{\text{ho}}(\omega_c, 0) & 0 \\ 0 & H_{\text{MS}}^{\text{ho}}(\omega_c, 0) \end{pmatrix} - \hbar \frac{g^2}{\omega_c},$$

$$B = \begin{pmatrix} 0 & e^{ig\sqrt{\frac{s}{\hbar\omega_c}}\hat{x}} \\ e^{-ig\sqrt{\frac{s}{\hbar\omega_c}}\hat{x}} & 0 \end{pmatrix} = e^{-ig\sqrt{\frac{s}{\hbar\omega_c}}\hat{x}} \sigma_- + e^{ig\sqrt{\frac{s}{\hbar\omega_c}}\hat{x}} \sigma_+,$$

we obtain the expression,

$$\tilde{H}_{\text{QR}} = A - \hbar \frac{\omega_a}{2} B. \quad (7)$$

The operator A describes the particle's confinement within the potential well of the harmonic oscillator. The operator $-\hbar \frac{\omega_a}{2} B$ determines the tunneling behavior of the particle through the wells, thereby governing the tunneling within our two-level-system approximation by incorporating a weighted phase factor,

$$\frac{\hbar\omega_a}{2} e^{\pm ig\sqrt{\frac{s}{\hbar\omega_c}}\hat{x}}. \quad (8)$$

Thus, the particles acquire this phase factor as they pass through the barrier, such as a tunnel junction [38–41].

In addition to the appearance of the phase factor, as seen by comparing Eq.(3) and Eq.(7), we note that the tunneling does not change the effect of the harmonic-oscillator potential. The Schrödinger operator appearing in the diagonal elements (i.e., the (1, 1)- and (2, 2)-elements) of Eq.(4) can be rewritten as

$$H_{\text{MS}}^{\text{ho}}(\omega_c, 0) \pm g\sqrt{2\hbar\omega_c}\hat{x} = \frac{1}{2}\hat{p}^2 + \frac{\omega_c^2}{2} \left(\hat{x} \pm \frac{g}{\omega_c} \sqrt{\frac{2\hbar}{\omega_c}} \right)^2 - \hbar \frac{g^2}{\omega_c}. \quad (9)$$

Therefore, this fact indicates that the tunneling in the two-level-system approximation using the quantum Rabi model does not change the shape of the two wells of the harmonic oscillator potential, but merely shifts the positions of the potential minima and generates the self-energy $-\hbar \frac{g^2}{\omega_c}$.

In Ref.[43], the author introduced the unitary transformation analogous to $U_0 U_1 U_\phi$ solely as a purely mathematical construct; however, the above description provides a physical interpretation. This interpretation suggests that the ground-state energy expression of the spin-boson model [43] reflects the effects of a dilute instanton gas [44].

III. QUANTUM RABI MODEL AND TRANSITION TO SPONTANEOUS \mathbb{Z}_2 -SYMMETRY BREAKING

In this section, we introduce two limits that lead the quantum Rabi model to spontaneous \mathbb{Z}_2 -symmetry breaking. It is the transformed quantum Rabi model that actually reveals the transition to this spontaneous \mathbb{Z}_2 -symmetry breaking.

We consider the following two types of limits.

(LMT1) Fixing the frequencies ω_a and ω_c , we treat the coupling strength g as a parameter and take the limit $g \rightarrow \infty$.

(LMT2) Fixing the frequency ω_c , we introduce a variable r with $0 \leq r \leq 1$ and define the frequency ω_a and the coupling strength g as continuous functions of the variable r , i.e., $\omega_a = \omega_a(r)$ and $g = g(r)$. These functions satisfy the conditions, $\omega_a(r) \neq 0$ for $0 \leq r < 1$, $\omega_a(1) = 0$, $g(0) = 0$, and $g(r) \neq 0$ for $0 < r \leq 1$. We then take the limit $r \rightarrow 1$.

We denote by \lim_{SB} the limit given by (LMT1) or (LMT2). In the limit (LMT1), we recall that the parameter g represents the distance between the two minima of the symmetrical wells [2] (also see Eq.(9)). Therefore, the adiabatic approximation becomes mathematically valid in the strong-coupling limit $g \rightarrow \infty$ [45], as the tunneling from one minimum to another is virtually impossible for sufficiently large g . Exploiting this, we can allow the frequency ω_a to assume the role of the coupling strength g , leading to the limit (LMT2). This approach was first employed experimentally by Cai *et al.* to realize the transition using an ion-trap simulator [12]. While the transition to spontaneous \mathbb{Z}_2 -symmetry breaking is obtainable in both limits for the quantum Rabi model, it does not occur in (LMT1) when the so-called A^2 -term (i.e., mass term) $\hbar C g^2 (a + a^\dagger)^2$ is added to the Hamiltonian, where C is an arbitrary non-zero constant. This is due to the divergence of the free boson Hamiltonian after renormalization via the Hopfield-Bogoliubov transformation [45]. In contrast, the transition remains achievable in (LMT2) [34].

We define the Hamiltonian of the renormalized quantum Rabi model as:

$$H_{\text{QR}}^{\text{ren}} = H_{\text{QR}} + \hbar \frac{g^2}{\omega_c}.$$

Correspondingly, its unitary transformation is given by

$$\tilde{H}_{\text{QR}}^{\text{ren}} = (U_0 U_1 U_\phi)^* H_{\text{QR}}^{\text{ren}} (U_0 U_1 U_\phi) = A + \hbar \frac{g^2}{\omega_c} - \hbar \frac{\omega_a}{2} B.$$

It is obvious that the operator $-\frac{\hbar\omega_a}{2}B$ converges to 0 in (LMT2). Meanwhile, regarding the expectation value of this operator for any state $|\#\rangle|\psi\rangle$, the weighted phase factors in Eq.(8) — appearing in the off-diagonal elements — yield individual vibration integrals of the form $\int_{-\infty}^{+\infty} e^{\pm ig\sqrt{\frac{8}{\hbar\omega_c}}x} |\psi(x)|^2 dx$. These vibration integrals converge to 0 in (LMT1) [33] since the vibrations become increasingly rapid as $g \rightarrow \infty$. More generally, for arbitrary wavefunctions $\varphi(x)$ and $\psi(x)$, the integrals $\int_{-\infty}^{+\infty} \varphi^*(x) e^{\pm ig\sqrt{\frac{8}{\hbar\omega_c}}x} \psi(x) dx$ vanish in (LMT1) by the Riemann-Lebesgue lemma. We mathematically justify this heuristic argument below. By combining these convergences with Eq.(7), and following the methods in Refs.[33, 34, 46], we can show that the difference between $H_{\text{QM}}^{\text{ren}}$ and $(U_0 U_1 U_\phi) H_{\text{b}} (U_0 U_1 U_\phi)^*$ converges to 0 in the norm resolvent sense (see the definition in Ref.[47], p.284):

$$\lim_{\text{SB}} \left\| \left(\tilde{H}_{\text{QM}}^{\text{ren}} - z \right)^{-1} - (H_{\text{b}} - z)^{-1} \right\|_{\text{op}} = 0 \quad (10)$$

for all $z \in \mathbb{C}$ with $\Im z \neq 0$, where $\|\cdot\|_{\text{op}}$ denotes the operator norm, and H_{b} stands for the free-boson Hamiltonian $1 \otimes \hbar\omega_c (a^\dagger a + \frac{1}{2})$. The norm resolvent convergence implies the convergence of the energy levels (see Theorems VIII 23 and VIII 24 of Ref.[47]). We denote the limit in Eq.(10) by

$$\lim_{\text{SB}} \tilde{H}_{\text{QR}}^{\text{ren}} = H_{\text{b}} \quad \text{or} \quad \lim_{\text{SB}} H_{\text{QM}}^{\text{ren}} \cong H_{\text{b}}. \quad (11)$$

For the parity operator P , we define the transformed parity operator \tilde{P} by $\tilde{P} = (U_0 U_1 U_\phi)^* P (U_0 U_1 U_\phi)$, and we have $\tilde{P} = -\sigma_x (-1)^{a^\dagger a}$. This is the parity operator for the tunneling and the boson number. Eq.(2) ensures the parity symmetry of the transformed quantum Rabi Hamiltonian:

$$[\tilde{H}_{\text{QR}}, \tilde{P}] = [\tilde{H}_{\text{QR}}^{\text{ren}}, \tilde{P}] = 0. \quad (12)$$

Meanwhile, it is obvious that the \mathbb{Z}_2 -symmetry,

$$[-\sigma_x, H_{\text{b}}] = 0, \quad (13)$$

holds. This implies the following \mathbb{Z}_2 -symmetry,

$$[\tilde{P}, H_{\text{b}}] = 0 \quad (14)$$

since $[a^\dagger a, H_{\text{b}}] = 0$. Moreover, the Hamiltonian H_{b} possesses degenerate ground states, $|\downarrow\rangle|0\rangle$ and $|\uparrow\rangle|0\rangle$. This surely implies the spontaneous \mathbb{Z}_2 -symmetry breaking. Thus, the limit in the sense of (LMT1) or (LMT2) drives the renormalized Hamiltonian $H_{\text{QR}}^{\text{ren}}$ toward spontaneous \mathbb{Z}_2 -symmetry breaking (see Figs.5 and 6). Eqs.(13) and

(14) then characterize the difference in \mathbb{Z}_2 -symmetry, reflecting the emergence of the single-mode boson (i.e., Bose quasi-particle) penetration:

$$\begin{cases} [\tilde{P}, \tilde{H}_{\text{QR}}^{\text{ren}}] = 0 = [-\sigma_x, \tilde{H}_{\text{QR}}^{\text{ren}}] & \text{in LMT1 or LMT2,} \\ [\tilde{P}, \tilde{H}_{\text{QR}}^{\text{ren}}] = 0 \neq [-\sigma_x, \tilde{H}_{\text{QR}}^{\text{ren}}] & \text{for } \frac{g}{\omega_a} < \infty. \end{cases} \quad (15)$$

The first commutation relation in Eq.(15) indicates that the tunneling between the bosonic states \mathcal{F}_\downarrow and the fermionic states \mathcal{F}_\uparrow is independent of the penetration of the single-mode boson (i.e., Bose quasi-particle). Once the tunneling is activated, it breaks one of the two \mathbb{Z}_2 -symmetries, as evidenced by $[-\sigma_x, \tilde{H}_{\text{QR}}^{\text{ren}}] \neq 0$ in Eq.(15). In contrast, the other \mathbb{Z}_2 -symmetry remains intact for all parameters, ω_a, ω_c , and g , as $[\tilde{P}, \tilde{H}_{\text{QR}}^{\text{ren}}] = 0$ in Eq.(15). This implies that the tunneling is assisted by the penetration of the single-mode boson.

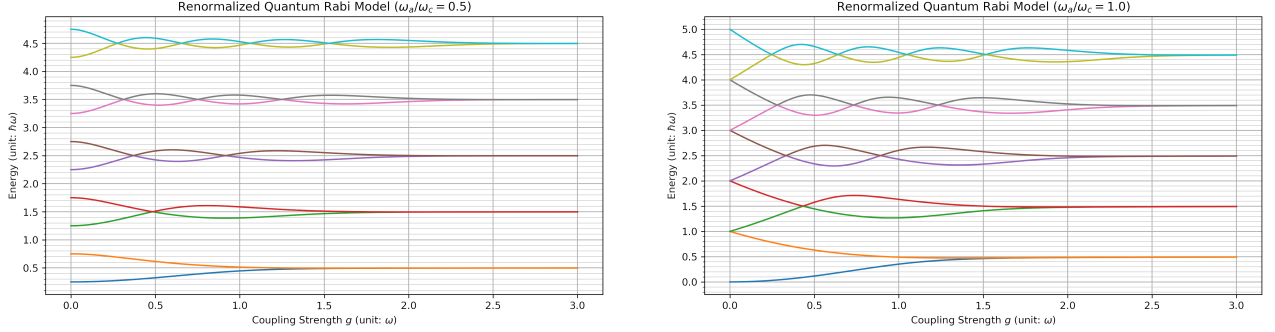


FIG. 5. The first ten energy levels of the renormalized quantum Rabi model in the limit (LMT1). The qubit transition frequency, the frequency of the single-mode boson, and the coupling strength between them are denoted by ω_a , ω_c , and g , respectively. For a constant frequency ω , the left panel shows the energy levels for $\omega_a = 0.5\omega$ and $\omega_c = \omega$, while the right panel displays the case where $\omega_a = \omega_c = \omega$. At $g = 0$, the $\mathcal{N} = 2$ SUSY is observed in the right graph, whereas it is absent in the left panel.

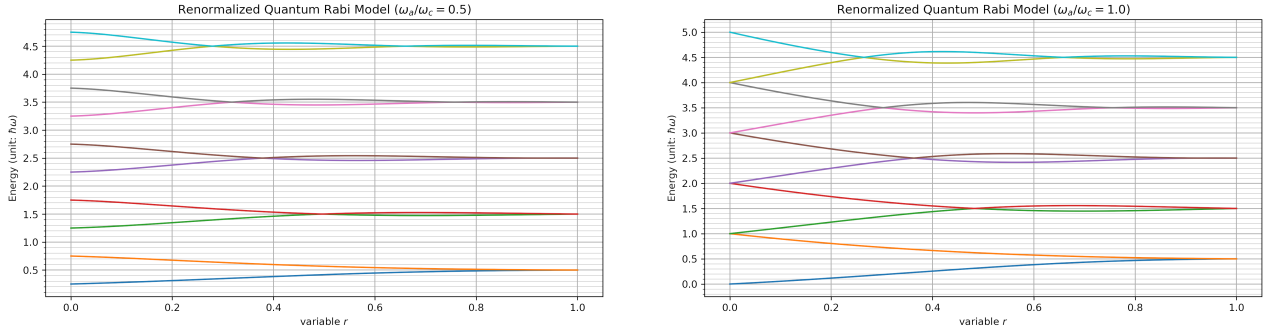


FIG. 6. The first ten energy levels of the renormalized quantum Rabi model in the limit (LMT2). Here, the qubit transition frequency, the frequency of the single-mode boson, and the coupling strength between the qubit and the boson are denoted by $\omega_a(r)$, ω_c , and $g(r)$ ($0 \leq r \leq 1$), respectively. For a constant frequency ω , the left panel shows the energy levels for $\omega_a(0) = 0.5\omega$ and $\omega_c = \omega$, while the right panel shows them for $\omega_a(0) = \omega_c = \omega$. At $r = 0$ (i.e., $g(0) = 0$), the $\mathcal{N} = 2$ SUSY can be found in the right panel, but not in the left panel.

We now tune the frequencies so that the strict condition, $\omega_a = \omega_c$, is satisfied. Since the quantum Rabi Hamiltonian H_{QR} with $g = 0$ corresponds to the so-called Witten Hamiltonian [48, 49], SUSY is obtained under this resonance condition, $\omega_a = \omega_c$ (see the right panels of Figs.5 and 6). It is worthy to note that the tuning of $\omega_a = \omega_c$ is straightforward in certain quantum simulators.

The anisotropic quantum Rabi model [50–54] describes the interaction between a qubit and a single-mode boson in a cavity. The interaction is defined by interpolating between the quantum Rabi model and the Jaynes-Cummings model, which breaks the balance between the rotating terms and the counter-rotating terms of the linear interaction. In the strong-coupling limit ($g \rightarrow \infty$), the anisotropic quantum Rabi model undergoes a transition to spontaneous \mathbb{Z}_2 -symmetry breaking that is stable against variations in the frequencies ω_a and ω_c , as well as the imbalance between rotating and counter-rotating terms [55]. Therefore, under the condition $\omega_a = \omega_c$, the anisotropic quantum Rabi

model exhibits a transition from the $\mathcal{N} = 2$ SUSY to its spontaneous breaking. However, this imbalance causes a mass reduction [55], as the tunneling effect induces momentum penetration (or, alternatively, position penetration according to Eq.5). Thus, it is worth studying another SUSY and its spontaneous breaking within the context of the anisotropic quantum Rabi model [56].

IV. OCCURRENCE OF POLYAKOV'S ENERGY BIFURCATION

In this section, we demonstrate the restoration of the spontaneously broken \mathbb{Z}_2 -symmetry in the (renormalized) quantum Rabi model, following Polyakov's statement [8].

Let us view this recovery as being in the opposite direction to the transition to spontaneous \mathbb{Z}_2 -symmetry breaking. When this spontaneous breaking occurs, the renormalized, transformed quantum Rabi Hamiltonian $\tilde{H}_{\text{QR}}^{\text{ren}}$ no longer possesses a tunneling interaction between the subspaces of bosonic and fermionic states, as shown in Eq.(11); consequently, it features degenerate ground states at $\frac{g}{\omega_a} = \infty$. Once $\frac{g}{\omega_a}$ becomes finite (i.e., $\frac{g}{\omega_a} < \infty$), the tunneling interaction emerges, and the Hamiltonian becomes to the full transformed quantum Rabi Hamiltonian. The (transformed) quantum Rabi Hamiltonian has a unique ground state [57], where the \mathbb{Z}_2 -symmetry is restored from spontaneous breaking. Thus, the degeneracy is lifted, and the degenerate ground state splits into the ground state and the first excited state (see, for instance, Figs.7, 8, and 9). We show below that this phenomenon originates from Polyakov's statement.

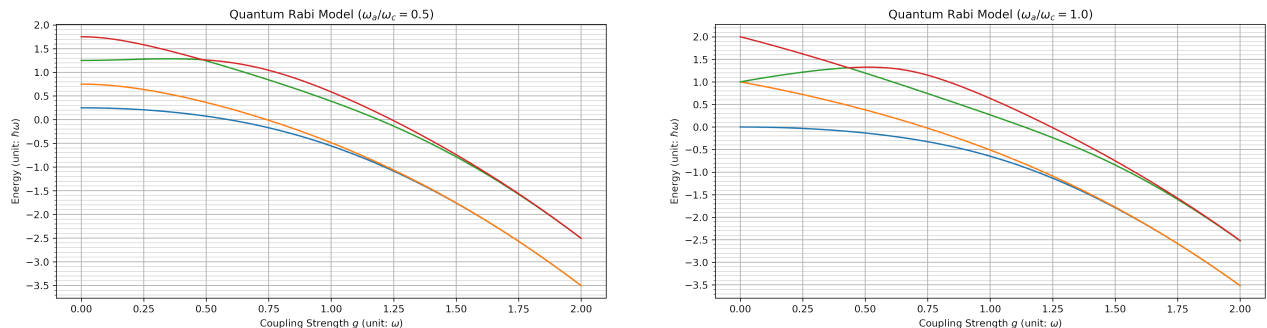


FIG. 7. The four lowest energy levels of the quantum Rabi model from (LMT1). Here, the qubit-transition frequency, the single-mode boson frequency, and the coupling strength between the qubit and the boson are denoted by ω_a , ω_c , and g , respectively. For a constant frequency ω , the left panel shows the energy levels in the cases $\omega_a = 0.5\omega$ and $\omega_c = \omega$, while the right panel shows the case $\omega_a = \omega_c = \omega$. At $g = 0$, we find the $\mathcal{N} = 2$ SUSY in the right panel, but not in the left one.

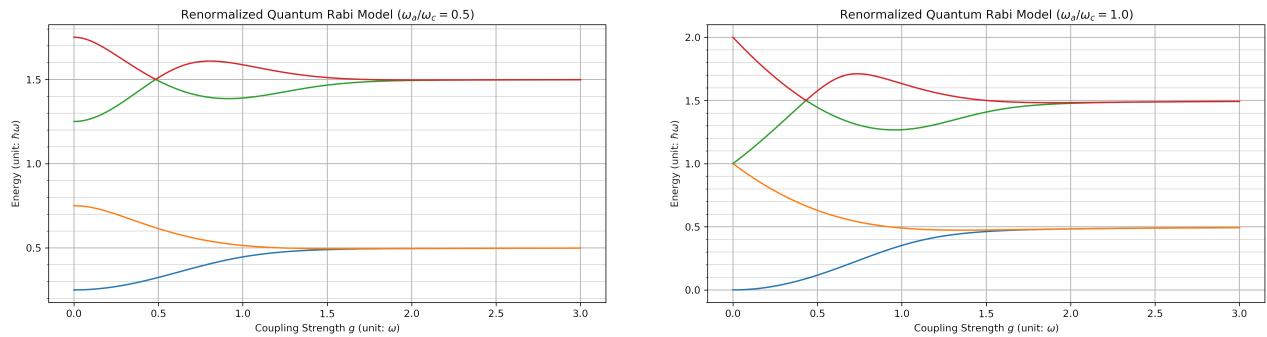


FIG. 8. The first four energy levels of the renormalized quantum Rabi model in (LMT1). Here, ω_a , ω_c , and g denote the qubit-transition frequency, the frequency of the single-mode boson, and the coupling strength between them, respectively. For a constant frequency ω , the left panel shows the energy levels for $\omega_a = 0.5\omega$ and $\omega_c = \omega$, while the right panel shows the case where $\omega_a = \omega_c = \omega$. At $g = 0$, the $\mathcal{N} = 2$ SUSY is observed in the right panel, but not in the left.

Thanks to the parity symmetry given by Eq.(12), the total state space $\mathbb{C}^2 \otimes \mathcal{F}_b$ can be decomposed into the direct sum $\mathcal{F}_+ \oplus \mathcal{F}_-$. Here, \mathcal{F}_\pm are the mutually orthogonal eigenspaces of the transformed parity operator \tilde{P} satisfying $\tilde{P}\mathcal{F}_\pm = \mp\mathcal{F}_\pm$. In other words, the eigenvalue equation $\tilde{P}|\psi_\pm\rangle = \mp|\psi_\pm\rangle$ holds for every $|\psi_\pm\rangle \in \mathcal{F}_\pm$. Correspondingly, the symmetry in Eq.(12) induces the Hamiltonian decomposition, $\tilde{H}_{\text{QR}} = \tilde{H}_+ + \tilde{H}_-$, where each \tilde{H}_\pm acts on the domain

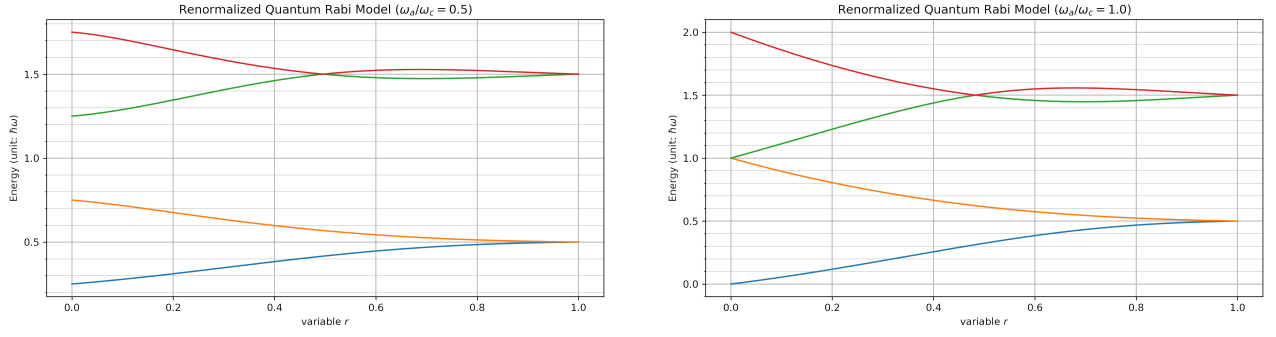


FIG. 9. Energy levels of the renormalized quantum Rabi model in (LMT2). The first four energy levels are shown. Here, $\omega_a(r)$, ω_c , and $g(r)$ denote the qubit-transition frequency, the frequency of the single-mode boson, and the coupling strength, respectively. For a constant frequency ω , the left panel shows the energy levels for $\omega_a(0) = 0.5\omega$ and $\omega_c = \omega$, while the right graph shows the case where $\omega_a(0) = \omega_c = \omega$. At $r = 0$ (i.e., $g(0) = 0$), we can find $\mathcal{N} = 2$ SUSY in the right panel, but not in the left one.

$\text{Dom}(\tilde{H}_{\pm}) \subset \mathcal{F}_{\pm}$ and leaves the subspace \mathcal{F}_{\pm} invariant, i.e., $\tilde{H}_{\pm}\text{Dom}(\tilde{H}_{\pm}) \subset \mathcal{F}_{\pm}$. We denote this decomposition by

$$\tilde{H}_{\text{QR}} = \tilde{H}_+ \oplus \tilde{H}_-. \quad (16)$$

Similarly to Eq.(2.18) of Ref.[43] or Eqs.(3.98) and (3.99) of Ref.[36], we define the states $\tilde{\Omega}_{\pm} = (|\uparrow\rangle|0\rangle \pm |\downarrow\rangle|0\rangle)/\sqrt{2}$ and $\tilde{\Omega}_{\pm} = (U_0 U_1 U_{\phi})\tilde{\Omega}_{\pm}$. It follows that $\tilde{\Omega}_{\pm} \in \mathcal{F}_{\pm}$, i.e., $\tilde{P}\tilde{\Omega}_{\pm} = \mp\tilde{\Omega}_{\pm}$. Based on the decomposition given by Eq.(16), we have

$$\langle \tilde{\Omega}_{\pm} | e^{-\beta\tilde{H}_{\text{QR}}}\tilde{\Omega}_{\pm} \rangle = \langle \tilde{\Omega}_{\pm} | e^{-\beta\tilde{H}_{\pm}}\tilde{\Omega}_{\pm} \rangle.$$

We define the constants E_{\pm} by

$$E_{\pm} = -\lim_{\beta \rightarrow \infty} \frac{1}{\beta} \ln \langle \tilde{\Omega}_{\pm} | e^{-\beta\tilde{H}_{\pm}}\tilde{\Omega}_{\pm} \rangle.$$

Following the arguments in Lemma 2.3 in Ref.[43], as adapted in Ref.[9], we obtain the expression

$$E_{\pm} = \frac{\hbar\omega_c}{2} - \frac{\hbar g^2}{\omega_c} \mp \frac{\hbar\omega_a}{2} \exp \left[-2\frac{g^2}{\omega_c^2} (G(g) + 1) \right], \quad (17)$$

where the quantity $G(g)$ depends on the coupling strength g and satisfies $-1 \leq G(g) \leq 0$. We consider a situation where neither the ground-state energy nor the first excited energy has any energy-level crossing for $0 < g < \infty$. It is noteworthy that there is no energy-level crossing between the ground and the first excited states [57]. As shown in Figs.4-8, we have such a situation provided that $0 < \omega_a \leq \omega_c$ and $0 < \frac{g}{\omega_a} < \infty$. At least mathematically, this situation occurs for sufficiently large $\frac{g}{\omega_a}$ [33, 34]. Due to the decomposition given by Eq.(16), the energies E_+ and E_- are respectively the ground-state energy E_0 and the first-excited-state energy E_1 of the transformed quantum Rabi Hamiltonian \tilde{H}_{QR} (and thus the quantum Rabi Hamiltonian H_{QR}) since $E_+ \leq E_-$: $E_0 = E_+$ and $E_1 = E_-$.

The expressions given in Eq.(17) are consistent with Polyakov's statement. As shown in Ref.[9], we obtain

$$S_{\text{euc}}(q_{\text{cl}}) = 2\hbar \frac{g^2}{\omega_c^2} (G(g) + 1) \quad (18)$$

for the classical Euclidean action $S_{\text{euc}}(q_{\text{cl}})$ of an effective instanton-like particle. For the renormalized quantum Rabi Hamiltonian $H_{\text{QR}}^{\text{ren}}$, Eqs.(17) and (18) yield the expressions for the ground-state energy E_0^{ren} and the first excited-state energy E_1^{ren} as

$$E_0^{\text{ren}} = \frac{\hbar\omega_c}{2} - \frac{\hbar\omega_a}{2} \exp \left[-\frac{S_{\text{euc}}(q_{\text{cl}})}{\hbar} \right] \quad (19)$$

and

$$E_1^{\text{ren}} = \frac{\hbar\omega_c}{2} + \frac{\hbar\omega_a}{2} \exp \left[-\frac{S_{\text{euc}}(q_{\text{cl}})}{\hbar} \right]. \quad (20)$$

The expressions in Eqs.(19) and (20) are similar to Eq. (12.68) of Ref.[36]. Based on the results in Refs.[9, 43], $G(g) \neq -1$ holds for every finite g ; consequently, we obtain the limit

$$\lim_{\text{SB}} \frac{\hbar\omega_a}{2} \exp \left[-\frac{S_{\text{euc}}(q_{\text{cl}})}{\hbar} \right] = \lim_{\text{SB}} \frac{\hbar\omega_a}{2} \exp \left[-2\frac{g^2}{\omega_c^2} (G(g) + 1) \right] = 0$$

(see Figs.7, 8, and 9). We find that the energy levels E_0^{ren} and E_1^{ren} form a degenerate ground state at $\frac{g}{\omega_a} = \infty$:

$$E_0^{\text{ren}} = \frac{\hbar\omega_c}{2} = E_1^{\text{ren}}. \quad (21)$$

On the other hand, once the ratio $\frac{g}{\omega_a}$ becomes finite (i.e., $\frac{g}{\omega_a} < \infty$), Polyakov's bifurcation takes place:

$$E_0^{\text{ren}} = \frac{\hbar\omega_c}{2} - \frac{\hbar\omega_a}{2} \exp \left[-\frac{S_{\text{euc}}(q_{\text{cl}})}{\hbar} \right] < \frac{\hbar\omega_c}{2} + \frac{\hbar\omega_a}{2} \exp \left[-\frac{S_{\text{euc}}(q_{\text{cl}})}{\hbar} \right] = E_1^{\text{ren}}.$$

In particular the inequality becomes $E_0^{\text{ren}} = \frac{\hbar\omega_c}{2} - \frac{\hbar\omega_a}{2} < \frac{\hbar\omega_c}{2} + \frac{\hbar\omega_a}{2} = E_1^{\text{ren}}$ at $\frac{g}{\omega_a} = 0$. Therefore, we can conclude that the tunneling term $\frac{\hbar\omega_a}{2} \exp \left[-\frac{S_{\text{euc}}(q_{\text{cl}})}{\hbar} \right]$ induced by the effective instanton-like particle is consistent with Polyakov's findings (see Figs.7, 8, and 9).

In experimental observations, energy level differences are typically detected through photon emission. It is therefore meaningful to express the classical Euclidean action $S_{\text{euc}}(q_{\text{cl}})$ in terms of the energy gap between the ground and first excited states. In the same way that Eq. (12.69) is derived in Ref.[36], Eqs.(19) and (20) lead to the expression

$$S_{\text{euc}}(q_{\text{cl}}) = -\hbar \ln \left[\frac{E_1^{\#} - E_0^{\#}}{\hbar\omega_a} \right], \quad (22)$$

where $E_i^{\#}$ is E_i or E_i^{ren} for $i = 0, 1$.

We, for example, set the double-well potential as $V(x) = C_{\text{dw}}(x^2 - q_0^2)^2$ with a positive constant C_{dw} . The classical Euclidean action for the macrosystem Hamiltonian H_{MS} , defined by Eq.(1), is then given by Eq.(2.22) of Ref.[26] or Eq. (3.36) of Ref.[44]; hence, we obtain the approximation

$$S_{\text{euc}}(q_{\text{cl}}) \approx \int_{-q_0}^{+q_0} \sqrt{2V(x)} dx.$$

This approximation and Eq.(22) yield

$$q_0 \approx \left\{ -\frac{3\hbar}{4\sqrt{2}C_{\text{dw}}} \ln \left[\frac{E_1^{\#} - E_0^{\#}}{\hbar\omega_a} \right] \right\}^{1/3}, \quad (23)$$

which reveals that the coordinates of the minima, $\pm q_0$, diverge from each other and tend to $\pm\infty$, respectively, in (LMT1), although further analysis of the behavior of the logarithmic term is necessary in (LMT2).

V. CONCLUSION AND DISCUSSION

We have demonstrated that the transformed quantum Rabi model effectively describes macroscopic quantum tunneling (MQT). Our mathematical analysis revealed that the bifurcation proposed by Polyakov arises for recovery from spontaneous symmetry breaking. This suggests that Polyakov's bifurcation is potentially observable in quantum simulations, which raises further questions regarding the realization and detectability of the effective instanton-like particle in such systems. Furthermore, we have shown that $\mathcal{N} = 2$ supersymmetry (SUSY) emerges as a special case of the reverse process of Polyakov's bifurcation.

Let us point out one specific problem regarding these questions. Since the term $\frac{\hbar\omega_a}{2} \exp \left[-\frac{S_{\text{euc}}(q_{\text{cl}})}{\hbar} \right]$ in Eqs.(19) and (20) vanishes in both (LMT1) and (LMT2), which implies Eq.(21), the tunneling of single-mode bosons disappears when spontaneous \mathbb{Z}_2 -symmetry breaking occurs. Regarding (LMT1), this vanishing mathematically occurs after taking the limit; however, as shown in Figs.5 and 8, the decay is rapid. We are interested in the behavior of the classical Euclidean action $S_{\text{euc}}(q_{\text{cl}})$, namely, the existence of instanton-like configurations, in these two limits. Furthermore, if such configurations exist, we must investigate how they lose their role in facilitating tunneling, as demonstrated,

for instance, by Eq.(23) in (LMT1). Meanwhile, the spontaneous \mathbb{Z}_2 -symmetry breaking should produce the Nambu-Goldstone fermion [48, 49, 58, 59]. We are also interested in whether a relation exists between the instanton-like configurations in (LMT1) or (LMT2) and the Nambu-Goldstone fermion [9, 34].

We expect that simulations based on the quantum Rabi model will provide a robust platform for investigating phenomena caused by instantons both theoretically and experimentally. These findings open up possibilities for extending the current framework to spin-boson models, potentially paving the way for further considerations in quantum field theory.

ACKNOWLEDGMENTS

This work was supported by the Quantum and Spacetime Research Institute (QuaSR), Kyushu University. The author thanks Shiro Saito and Yutaka Tabuchi for the fruitful discussions. This Perspective is dedicated to Pavel Exner, Herbert Spohn, and Valentin Zagrebnoy on the occasion of their 80th birthdays.

DATA AVAILABILITY

All energy spectra data in the figures can be generated using Python code with QuTiP [60, 61].

-
- [1] A. J. Leggett, Macroscopic quantum systems and the quantum theory of measurement, Progress of Theoretical Physics Supplement **69**, 80 (1980).
 - [2] A. J. Leggett, S. Chakravarty, A. T. Dorsey, M. P. A. Fisher, A. Garg, and W. Zwerger, Dynamics of the dissipative two-state system, Rev. Mod. Phys. **59**, 1 (1987).
 - [3] S. Takagi, *Macroscopic Quantum Tunneling* (Cambridge University Press, Cambridge, 2002).
 - [4] A. Caldeira and A. Leggett, Influence of dissipation on quantum tunneling in macroscopic systems, Phys. Rev. Lett. **46**, 211 (1981).
 - [5] M. H. Devoret, J. M. Martinis, D. Esteve, and J. Clarke, Resonant activation from the zero-voltage state of a current-biased josephson junction, Phys. Rev. Lett. **53**, 1260 (1984).
 - [6] J. M. Martinis, M. H. Devoret, and J. Clarke, Energy-level quantization in the zero-voltage state of a current-biased josephson junction, Phys. Rev. Lett. **55**, 1543 (1985).
 - [7] M. H. Devoret, J. M. Martinis, and J. Clarke, Measurements of macroscopic quantum tunneling out of the zero-voltage state of a current-biased josephson junction, Phys. Rev. Lett. **55**, 1908 (1985).
 - [8] A. M. Polyakov, Quark confinement and topology of gauge theories, Nucl. Phys. B **120**, 429 (1977).
 - [9] M. Hirokawa, Instanton-like effect caused by qubit-boson interaction in light of quantum simulation, Scientific Reports **15**, 37413 (2025).
 - [10] J. Braumüller, M. Marthaler, A. Schneider, A. Stehli, H. Rotzinger, M. Weides, and A. V. Ustinov, Analog quantum simulation of the Rabi model in the ultra-strong coupling regime, Nat. Commun. **8**, 779 (2017).
 - [11] M.-L. Cai, Z.-D. Liu, W.-D. Zhao, Y.-K. Wu, Q.-X. Mei, Y. Jiang, L. He, X. Zhang, Z.-C. Zhou, and L.-M. Duan, Observation of a quantum phase transition in the quantum rabi model with a single trapped ion, Nat. Commun. **12**, 5313 (2021).
 - [12] M.-L. Cai, Y.-K. Wu, Q.-X. Mei, W.-D. Zhao, Y. Jiang, L. Yao, L. He, Z.-C. Zhou, and L.-M. Duan, Observation of supersymmetry and its spontaneous breaking in a trapped ion quantum simulator, Nat. Commun. **13**, 3412 (2022).
 - [13] Z. Wu1, C. Hu, T. Wang, Y. Chen, Y. Li, L. Z. X.-Y. Lü, and X. Peng, Experimental quantum simulation of multicriticality in closed and open Rabi model, Phys. Rev. Lett. **133**, 173602 (2024).
 - [14] R. Gerritsma, B. P. Lanyon, G. Kirchmair, F. Zähringer, C. Hempel, J. Casanova, J. J. García-Ripoll, E. Solano, R. Blatt, and C. F. Roos, Quantum simulation of the Klein paradox with trapped ions, Phys. Rev. Lett. **106**, 060503 (2011).
 - [15] M. Endres, T. Fukuhara, D. Pekker, M. Cheneau, P. Schauß, C. Gross, E. Demler, S. Kuhr, and I. Bloch, The ‘Higgs’ amplitude mode at the two-dimensional superfluid/Mott insulator transition, Nature **487**, 454 (2012).
 - [16] D. Yang, G. S. Giri, M. Johanning, C. Wunderlich, P. Zoller, and P. Hauke, Analog quantum simulation of (1 + 1)-dimensional lattice QED with trapped ions, Phys. Rev. A **94**, 052321 (2016).
 - [17] E. A. Martinez, C. A. Muschik, P. Schindler, D. Nigg, A. Erhard, M. Heyl, P. Hauke, M. Dalmonte, T. Monz, P. Zoller, and R. Blatt, Real-time dynamics of lattice gauge theories with a few-qubit quantum computer, Nature **534**, 516 (2016).
 - [18] C. Kokail, C. Maier, R. van Bijnen, T. Brydges, M. K. Joshi, P. Jurcevic, C. A. Muschik, P. Silvi, R. Blatt, C. F. Roos, and P. Zoller, Self-verifying variational quantum simulation of lattice models, Nature **569**, 355 (2019).
 - [19] C. Schweizer, F. Grusdt, M. Berngruber, L. Barbiero, E. Demler, N. Goldman, I. Bloch, and M. Aidelsburger, Floquet approach to \mathbb{Z}_2 lattice gauge theories with ultracold atoms in optical lattices, Nat. Phys. **15**, 1168 (2019).
 - [20] B. Yang, H. Sun, R. Ott, H.-Y. Wang, T. V. Zache, J. C. Halimeh, Z.-S. Yuan, P. Hauke, and J.-W. Pan, Observation of gauge invariance in a 71-site Bose-Hubbard quantum simulator, Nature **587**, 392 (2020).

- [21] X. Zhang, W. Jiang, J. Deng, K. Wang, J. Chen, P. Zhang, W. Ren, H. Dong, S. Xu, Y. Gao, F. Jin, X. Zhu, Q. Guo, H. Li, C. Song, A. V. Gorshkov, T. Iadecola, F. Liu, Z.-X. Gong, Z. Wang, D.-L. Deng, and H. Wang, Digital quantum simulation of floquet symmetry-protected topological phases, *Nature* **607**, 468 (2022).
- [22] B. Wehinger, F. T. Lisandrini, N. Kestin, P. Bouillot, S. Ward, B. Thielemann, R. Bewley, M. Boehm, D. Biner, K. W. Krämer, B. Normand, T. Giamarchi, C. Kollath, A. M. Läuchli, and C. Rüegg, Fingerprints of supersymmetric spin and charge dynamics observed by inelastic neutron scattering, *Nat. Commun.* **16**, 3228 (2025).
- [23] D. González-Cuadra, M. Hamdan, T. V. Zache, B. Braverman, M. Kornjača, A. Lukin, S. H. Cantú, F. Liu, S.-T. Wang, A. Keesling, M. D. Lukin, P. Zoller, and A. Bylinskii, Observation of string breaking on a $(2 + 1)$ D Rydberg quantum simulator, *Nature* **642**, 321 (2025).
- [24] S. Coleman, Fate of the false vacuum: Semiclassical theory, *Phys. Rev. D* **15**, 2929 (1977).
- [25] C. G. Callan and S. Coleman, Fate of the false vacuum. II. first quantum corrections, *Phys. Rev. D* **16**, 1762 (1977).
- [26] S. Coleman, *The uses of instantons. In Aspects of Symmetry: Selected Erice Lectures* (Cambridge University Press, Cambridge, 1985) pp. 265–350.
- [27] R. P. Feynman, R. B. Leighton, and M. Sands, *Quantum field theory in a nutshell* (Addison-Wesley Publishing Company, Massachusetts, 1965).
- [28] F. Hund, Zur Deutung der Molekelspektren. I, *Zeits. für Phys.* **40**, 742 (1927).
- [29] F. Hund, Zur Deutung der Molekelspektren. II, *Zeits. für Phys.* **42**, 93 (1927).
- [30] F. Hund, Zur Deutung der Molekelspektren. III, *Zeits. für Phys.* **43**, 805 (1927).
- [31] A. S. Wightman and N. Glance, Superselection rules in molecules, *Nucl. Phys. B - Proceedings Supplements* **6**, 202 (1989).
- [32] J. Trost and K. Hornberger, Hund’s paradox and the collisional stabilization of chiral molecules, *Phys. Rev.Lett.* **103**, 023202 (200).
- [33] M. Hirokawa, The Rabi model gives off a flavor of spontaneous SUSY breaking, *Quantum Stud.: Math. Found.* **2**, 379 (2015).
- [34] M. Hirokawa, Can quantum rabi model with A^2 -term avoid no-go theorem and make quantum simulation of mass-enhancement in susy breaking?, *Quantum Stud.: Math. Found.* **11**, 673 (2024).
- [35] A. Caldeira and A. Leggett, Quantum tunnelling in a dissipative system, *Ann. Phys. (N.Y.)* **149**, 374 (1983).
- [36] M. Razavy, *Quantum Theory of Tunneling* (World Scientific, New Jersey, 2003).
- [37] Y. Nakamura and J. S. Tsai, A coherent two-level system in a superconducting single-electron transistor observed through photon-assisted cooper-pair tunneling, *J. Superconductivity* **12**, 799 (1999).
- [38] Y. Furuhashi, M. Hirokawa, K. Nakahara, and Y. Shikano, Role of phase factor in boundary condition of one-dimensional junction, *Journal of Physics A: Mathematical and Theoretical* **43**, 354010 (2010).
- [39] Y. Shikano and M. Hirokawa, Boundary conditions in one-dimensional tunneling junction, *Journal of Physics: Conference Series* **302**, 0124044 (2011).
- [40] M. Hirokawa and T. Kosaka, One-dimensional tunnel-junction formula for schrödinger particle, *SIAM Journal on Applied Mathematics* **73**, 2247 (2013).
- [41] M. Hirokawa and T. Kosaka, A mathematical aspect of a tunnel-junction for spintronic qubit, *Journal of Mathematical Analysis and Applications* **417(2)**, 856 (2014).
- [42] S. Albeverio, F. Gesztesy, R. Hoegh-Krohn, and H. Holden, *Solvable Models in Quantum Mechanics* (Springer, Berlin, 1988).
- [43] M. Hirokawa, An expression of the ground state energy of the spin-boson model, *J. Funct. Anal.* **162**, 178 (1999).
- [44] A. Altland and B. Simons, *Condensed Matter Field Theory, 2nd edition* (Cambridge University Press, New York, 2010).
- [45] M. Hirokawa, Srödinger-cat-like states with dressed photons in renormalized adiabatic approximation for generalized quantum Rabi Hamiltonian with quadratic interaction, *Physics Open* **5**, 100039 (2020).
- [46] M. Hirokawa, J. S. Møller, and I. Sasaki, A mathematical analysis of dressed photon in ground state of generalized quantum Rabi model using pair theory, *J. Phys. A: Math. Theo.* **50**, 184003 (2017).
- [47] M. Reed and B. Simon, *Methods of modern mathematical physics I: Functional analysis* (Academic Press, San Diego, 1980).
- [48] E. Witten, Dynamical breaking of supersymmetry, *Nucl. Phys. B* **185**, 513 (1981).
- [49] E. Witten, Constraints on supersymmetry breaking, *Nucl. Phys. B* **202**, 253 (1982).
- [50] M. Tomka, O. E. Araby, M. Pletyukhov, and V. Gritsev, Exceptional and regular spectra of a generalized Rabi model, *Phys. Rev. A* **90**, 063839 (2014).
- [51] L.-T. Shen, Z.-B. Yang, M. Lu, R.-X. Chen, and H.-Z. Wu, Ground state of the asymmetric Rabi model in the ultrastrong coupling regime, *Appl. Phys. B* **117**, 195 (2014).
- [52] Q.-T. Xie, S. Cui, J.-P. Cao, L. Amico, and H. Fan, Anisotropic rabi model, *Phys. Rev. X* **4**, 021046 (2014).
- [53] G. Zhang and H. Zhu, Analytical solution for the anisotropic Rabi model: Effects of counter-rotating terms, *Sci. Rep.* **5**, 8756 (2015).
- [54] G. Wang, R. Xiao, H. Z. Shen, C. Sun, and K. Xue, Simulating anisotropic quantum rabi model via frequency modulation, *Scientific Reports* **9**, 4569 (2019).
- [55] M. Hirokawa, F. Hiroshima, and D.-Y. Lee, Asymptotics for anisotropic Rabi models, *arXiv:2510.20201* (2025).
- [56] A. Kafuri, F. H. Maldonado-Villamizar, A. Moroz, and B. M. Rodríguez-Lara, Supersymmetry journey from the Jaynes-Cummings to the anisotropic Rabi model, *J. Opt. Soc. Am.* **41**, C82 (2024).
- [57] M. Hirokawa and F. Hiroshima, Absence of energy level crossing for the ground state energy of the Rabi model, *Commun. Stoch. Anal.* **8**, 551 (2014).
- [58] D. Volkov and V. Akulov, Is the neutrino a goldstone particle?, *Phys. Lett. B* **46**, 109 (1973).
- [59] A. Salam and J. Strathdee, On goldstone fermions, *Phys. Lett. B* **49**, 465 (1974).

- [60] J. R. Johansson, P. D. Nation, and F. Nori, Qutip: An open-source Python framework for the dynamics of open quantum systems, *Comp. Phys. Commun.* **183**, 1760 (2012).
- [61] J. R. Johansson, P. D. Nation, and F. Nori, Qutip 2: A Python framework for the dynamics of open quantum systems, *Comp. Phys. Commun.* **184**, 1234 (2013).